A continuum elastic three-dimensional model for natural frequencies of single-walled carbon nanotubes

(Article begins on next page)

19 April 2024

A continuum elastic three-dimensional model for natural frequencies of single-walled carbon nanotubes

Salvatore Brischetto[*]

Abstract

The free vibration analysis of Single-Walled Carbon NanoTubes (SWCNTs) is proposed in the present paper. A continuum approach (based on an exact elastic three-dimensional shell model) is used for natural frequency investigation of simply supported SWCNTs. In order to apply this continuum model, carbon nanotubes are defined as isotropic cylinders with an equivalent thickness and Young modulus. Preliminary remarks are proposed concerning the possible use of a continuum approach and the most convenient definitions of the equivalent thickness and Young modulus. Subsequently, the 3D shell method is compared with different beam analyses to show the limitations of 1D beam models. Finally, zigzag, armchair and general chirality SWCNTs (with various lengths and geometries) are analyzed via the 3D shell model to calculate their vibration modes.

Keywords: A. Nano-structures; B. Vibration; C. Analytical modelling; C. Numerical analysis.

1 Introduction

Carbon NanoTubes (CNTs) were discovered in Japan by Iijma [1] in 1991. CNTs are closed graphene sheets with a cylindrical shape. Research has shown that carbon nanotubes exhibit exceptional mechanical properties [2]. The elastic modulus has been shown to be greater than 1 TPa and the tensile

---

[*]Corresponding author: Salvatore Brischetto, Department of Mechanical and Aerospace Engineering, Politecnico di Torino, Corso Duca degli Abruzzi, 24, 10129 Torino, ITALY. tel: +39.011.090.6813, fax: +39.011.090.6899, e.mail: salvatore.brischetto@polito.it.

strength exceeds that of steel by over one order of magnitude. In view of their exceptional mechanical properties, CNTs are considered to be ideal reinforcements in composite structures [3]. Most CNT applications depend on their exceptional elastic properties. Therefore, it is of central importance to accurately quantify the elastic properties of Single-Walled CNTs (SWCNTs) [4] when a continuum elastic model is applied for their analysis.

Three basic methods are used to simulate the behavior of CNTs [5]: Molecular Dynamics (MD) simulations, atomistic-based modelling approaches and continuum approaches. In the former, the simulations are based on the definition of a potential energy function (e.g., Tersoff-Brenner or Lennard-Jones functions) [6]-[11]. In the second approach, CNTs are investigated using an atomistic finite element model with beam elements and concentrated masses. The beams simulate the interatomic covalent forces and the masses are located at the ends of the beams and represent the carbon positions [12]-[17]. The third approach considers carbon nanotubes (which have a discrete molecular structure) as continuum isotropic elastic cylinders which can be analyzed via beam or shell models. The computational effort necessary for the MD approach does not allow fast simulations of complex CNT networks. Simulations of a real size multi-walled CNT by means of an atomistic-based modelling approach are also expensive. Consequently, continuum approaches are preferred to MD and atomistic-based models in the described simulations because the computational cost is better. A carbon nanotube has a discrete molecular structure. Therefore, in order to apply a continuum model, it is necessary to correctly suppose its effective wall thickness, Young modulus and Poisson ratio. Extensive studies [18]-[21] have been conducted to analyze this feature, but a final conclusion has not yet been reached. In fact, the thickness and Young modulus values shown in the papers analyzed below are very different for the same elastic stiffness considered.

Many researchers have used beam models for continuum approaches to analyze free vibrations of single-walled carbon nanotubes. Among these, Santos [22] used finite elements based on the Euler-Bernoulli and Timoshenko beam theories. Azrar et al. [23] proposed the Timoshenko beam model with generalized boundary conditions in order to take into account a more realistic and wider range of boundary conditions. Unlike the Euler-Bernoulli beam model, the Timoshenko beam model allows for the effects of transverse shear deformation and rotary inertia [24]. The Discrete singular convolution (DSC) method based on the Timoshenko beam theory was used in [25] for free vibration problems of carbon nanotubes. Foda [26] proposed a direct analytical approach to suppress the steady state vibrations of a nanotube resting on a Winkler foundation. The natural frequencies and transversal

responses of simply supported single-walled carbon nanotubes were analyzed in [27] by means of the Timoshenko beam theory and the Bernoulli-Fourier method. Ming and Huiming [28] developed a single beam model to analyze the thermal vibration of SWCNTs. In this work nonlocal elasticity incorporated the effects of small size into the formulation. The flexural vibration of single-walled carbon nanotubes was analyzed in [29] by the finite element method. The Timoshenko beam element formulation was used for this purpose. Based on the nonlocal continuum theory, the nonlinear vibration of a SWCNT (considered as a curved beam subjected to a harmonic load) was investigated in [30]. Vibrations of nanotubes embedded in an elastic matrix were investigated in [31] by using the nonlocal Timoshenko beam model. Both a stress gradient and a strain gradient approach were considered. The transverse vibration of a single-walled carbon nanotube with light waviness along its axis was modeled in [32] by the nonlocal Euler-Bernoulli and Timoshenko beam theories. The comparison between the two models shows that the effects of transverse shear deformation and rotary inertia are considered only in the Timoshenko beam model. The nonlocal Euler-Bernoulli beam theory was used in [33] for forced vibrations of a simply supported single-walled carbon nanotube subjected to a moving harmonic load. Murmu and Pradhan [34] developed a nonlocal elasticity and though the Timoshenko beam theory investigated the stability response of a SWCNT embedded in an elastic medium. For the first time, both Winkler-type and Pasternak-type foundation models were employed to simulate the interaction of the SWCNT with the surrounding elastic medium. Non local constitutive equations of Eringen were used in [35], different beam theories including those of Euler-Bernoulli, Timoshenko, Reddy, Levinson and Aydogdu were compared.

The papers concerning the use of shell models for the vibration analysis of SWCNTs are less numerous than those concerning the beam models. Shell models are usually more complicated than beam models but they allow the analysis of CNTs with low length/diameter ratios. For these structures the use of 1D beam models gives significant errors because short CNTs are not one-dimensional structures. 2D or 3D shell models are suitable for the analysis of short CNTs. When the radius/thickness ratio is small, the use of refined 2D or 3D shell models are necessary for a correct vibration analysis as demonstrated in Cinefra et al. [36]. Wang and Zhang [37] proposed a two-dimensional elastic shell model to characterize the deformation of single-walled carbon nanotubes using the in-plane rigidity, Poisson ratio, bending rigidity and off-plane torsion rigidity as independent elastic constants. An elastic shell model of single-walled carbon nanotubes can be established only with a well-defined effective thickness. Vibrations of single-walled carbon nanotubes based on a three-dimensional theory of elasticity were an-

alyzed in [38]. The Flügge type shell equations (including the initial membrane hoop and axial stresses) were used in [39] as governing equations for free axisymmetric vibrations of a single-walled carbon nanotube. Dong et al. [40] presented an analytical laminated cylindrical shell method to investigate wave propagation in individual multiwall carbon nanotubes (MWNTs) or MWNTs embedded in an elastic matrix. Further shell models for Double-Walled Carbon NanoTubes (DWCNTs) were proposed in [41] and in [42] for free vibration and buckling analysis, respectively.

An exact three-dimensional elastic shell model is proposed in the present paper for free vibration analysis of simply supported SWCNTs. The equilibrium equations in general orthogonal curvilinear coordinates (see [43] and [44]) are developed for the case of a cylinder by giving an infinite value for one of the two radii of curvature. These equations are exactly solved by imposing harmonic forms for displacement components. The present model is validated by means of a comparison with the beam models given in [33] and [35]. Different length/diameter ratios are analyzed to understand the limitations of 1D beam models. Afterwards, the 3D shell model is used for the analysis of vibration modes of different zigzag, armchair and general chirality SWCNTs. Particular attention is given to the definition of the equivalent elastic properties of CNTs which actually are discrete molecular structures.

2   3D shell model

The three differential equations of equilibrium written for the case of free vibration analysis of multilayered spherical shells with constant radii of curvature R_α and R_β have been proposed in [43] and [44] where they have been solved in exact form in analogy with the method proposed in [45] and [46]. In this paper, the equations are simplified for the cylindrical case by imposing an infinite value for the radius of curvature R_β (see Fig. 1). The general form proposed in [43] and [44] remains valid for both plate and constant radius shell geometries.

2.1   Constitutive and geometrical relations

Three-dimensional linear elastic constitutive equations in orthogonal curvilinear coordinates (α, β, z) (see Fig. 1) are here given for a generic k isotropic layer. The stress components ($\sigma_{\alpha\alpha}$, $\sigma_{\beta\beta}$, σ_{zz}, $\sigma_{\beta z}$, $\sigma_{\alpha z}$, $\sigma_{\alpha\beta}$) are linked with the strain components ($\epsilon_{\alpha\alpha}$, $\epsilon_{\beta\beta}$, ϵ_{zz}, $\gamma_{\beta z}$, $\gamma_{\alpha z}$, $\gamma_{\alpha\beta}$) for each k isotropic layer

as:

$$\sigma_{\alpha\alpha k} = C_{11k}\epsilon_{\alpha\alpha k} + C_{12k}\epsilon_{\beta\beta k} + C_{13k}\epsilon_{zzk} \ , \tag{1}$$

$$\sigma_{\beta\beta k} = C_{12k}\epsilon_{\alpha\alpha k} + C_{22k}\epsilon_{\beta\beta k} + C_{23k}\epsilon_{zzk} \ , \tag{2}$$

$$\sigma_{zzk} = C_{13k}\epsilon_{\alpha\alpha k} + C_{23k}\epsilon_{\beta\beta k} + C_{33k}\epsilon_{zzk} \ , \tag{3}$$

$$\sigma_{\beta zk} = C_{44k}\gamma_{\beta zk} \ , \tag{4}$$

$$\sigma_{\alpha zk} = C_{55k}\gamma_{\alpha zk} \ , \tag{5}$$

$$\sigma_{\alpha\beta k} = C_{66k}\gamma_{\alpha\beta k} \ . \tag{6}$$

The strain-displacement relations of three-dimensional theory of elasticity in orthogonal curvilinear coordinates are written for the generic k layer of the multilayered cylindrical shell of Fig. 1 (the general form for spherical shells with constant radii of curvature R_α and R_β has been given in [43] and [44]):

$$\epsilon_{\alpha\alpha k} = \frac{1}{H_\alpha}u_{k,\alpha} + \frac{w_k}{H_\alpha R_\alpha} \ , \tag{7}$$

$$\epsilon_{\beta\beta k} = v_{k,\beta} \ , \tag{8}$$

$$\epsilon_{zzk} = w_{k,z} \ , \tag{9}$$

$$\gamma_{\beta zk} = w_{k,\beta} + v_{k,z} \ , \tag{10}$$

$$\gamma_{\alpha zk} = \frac{1}{H_\alpha}w_{k,\alpha} + u_{k,z} - \frac{u_k}{H_\alpha R_\alpha} \ , \tag{11}$$

$$\gamma_{\alpha\beta k} = \frac{1}{H_\alpha}v_{k,\alpha} + u_{k,\beta} \ . \tag{12}$$

The parametric coefficients for cylindrical shells are:

$$H_\alpha = (1 + \frac{z}{R_\alpha}) \ , \quad H_\beta = 1 \ , \quad H_z = 1 \ , \tag{13}$$

H_α depends on the z coordinate. $H_\beta = 1$ and $H_z = 1$ because β and z are rectilinear coordinates. R_α is the principal radius of curvature along the α coordinate. R_β is infinite for a cylinder (see Fig. 1). Partial derivatives $\frac{\partial}{\partial\alpha}$, $\frac{\partial}{\partial\beta}$ and $\frac{\partial}{\partial z}$ are indicated with subscripts $_{,\alpha}$, $_{,\beta}$ and $_{,z}$.

2.2 Equilibrium equations

The three differential equations of equilibrium written for the case of free vibration analysis of cylindrical shells are given (the most general form for spherical shells with constant radii of curvature can be found in [43] and [44]):

$$\sigma_{\alpha\alpha k,\alpha} + H_\alpha \sigma_{\alpha\beta k,\beta} + H_\alpha \sigma_{\alpha z k,z} + \frac{2}{R_\alpha} \sigma_{\alpha z k} = \rho_k H_\alpha \ddot{u}_k \ , \tag{14}$$

$$\sigma_{\alpha\beta k,\alpha} + H_\alpha \sigma_{\beta\beta k,\beta} + H_\alpha \sigma_{\beta z k,z} + \frac{1}{R_\alpha} \sigma_{\beta z k} = \rho_k H_\alpha \ddot{v}_k \ , \tag{15}$$

$$\sigma_{\alpha z k,\alpha} + H_\alpha \sigma_{\beta z k,\beta} + H_\alpha \sigma_{z z k,z} - \frac{1}{R_\alpha} \sigma_{\alpha\alpha k} + \frac{1}{R_\alpha} \sigma_{z z k} = \rho_k H_\alpha \ddot{w}_k \ , \tag{16}$$

where ρ_k is the mass density. $(\sigma_{\alpha\alpha k}, \sigma_{\beta\beta k}, \sigma_{zzk}, \sigma_{\beta zk}, \sigma_{\alpha zk}, \sigma_{\alpha\beta k})$ are the six stress components and $\ddot{u}_k$, $\ddot{v}_k$ and $\ddot{w}_k$ indicate the second temporal derivative of the three displacement components u_k, v_k and w_k, respectively. Each quantity depends on the k layer. R_α is referred to the mid-surface Ω_0 of the whole multilayered shell. H_α continuously varies through the thickness of the multilayered shell and it depends on the z thickness coordinate. Eqs.(14)-(16) have constant coefficients (even if a shell geometry is considered) when the shell is divided in $N_L = 230$ mathematical layers where the parametric coefficient H_α can easily be calculated in the middle of each k mathematical layer.

The closed form of Eqs.(14)-(16) is obtained for simply supported shells. The three displacement components have the following harmonic form:

$$u_k(\alpha,\beta,z,t) = U_k(z)e^{i\omega t}cos(\bar{\alpha}\alpha)sin(\bar{\beta}\beta) \ , \tag{17}$$

$$v_k(\alpha,\beta,z,t) = V_k(z)e^{i\omega t}sin(\bar{\alpha}\alpha)cos(\bar{\beta}\beta) \ , \tag{18}$$

$$w_k(\alpha,\beta,z,t) = W_k(z)e^{i\omega t}sin(\bar{\alpha}\alpha)sin(\bar{\beta}\beta) \ , \tag{19}$$

where $U_k(z)$, $V_k(z)$ and $W_k(z)$ are the displacement amplitudes in α, β and z directions, respectively. i is the coefficient of the imaginary unit. $\omega = 2\pi f$ is the circular frequency where f is the frequency value, t is the time. In coefficients $\bar{\alpha} = \frac{p\pi}{a}$ and $\bar{\beta} = \frac{q\pi}{b}$, p and q are the half-wave numbers and a and b are the shell dimensions in α and β directions, respectively (they are calculated in the mid-surface Ω_0).

Eqs.(1)-(6), (7)-(12) and (17)-(19) are substituted in Eqs.(14)-(16) to obtain the following system

of equations for each k mathematical layer:

$$\left(-\frac{C_{55k}}{H_\alpha R_\alpha^2} - \bar{\alpha}^2 \frac{C_{11k}}{H_\alpha} - \bar{\beta}^2 C_{66k} H_\alpha + \rho_k H_\alpha \omega^2\right) U_k + \left(-\bar{\alpha}\bar{\beta} C_{12k} - \bar{\alpha}\bar{\beta} C_{66k}\right) V_k + \left(\bar{\alpha}\frac{C_{11k}}{H_\alpha R_\alpha} + \right.$$

$$\left. \bar{\alpha}\frac{C_{55k}}{H_\alpha R_\alpha}\right) W_k + \left(\frac{C_{55k}}{R_\alpha}\right) U_{k,z} + \left(\bar{\alpha} C_{13k} + \bar{\alpha} C_{55k}\right) W_{k,z} + \left(C_{55k} H_\alpha\right) U_{k,zz} = 0 \,, \tag{20}$$

$$\left(-\bar{\alpha}\bar{\beta} C_{66k} - \bar{\alpha}\bar{\beta} C_{12k}\right) U_k + \left(-\bar{\alpha}^2 \frac{C_{66k}}{H_\alpha} - \bar{\beta}^2 C_{22k} H_\alpha + \rho_k H_\alpha \omega^2\right) V_k + \left(\bar{\beta}\frac{C_{44k}}{R_\alpha} + \bar{\beta}\frac{C_{12k}}{R_\alpha}\right) W_k +$$

$$\left(\frac{C_{44k}}{R_\alpha}\right) V_{k,z} + \left(\bar{\beta} C_{44k} H_\alpha + \bar{\beta} C_{23k} H_\alpha\right) W_{k,z} + \left(C_{44k} H_\alpha\right) V_{k,zz} = 0 \,, \tag{21}$$

$$\left(\bar{\alpha}\frac{C_{55k}}{H_\alpha R_\alpha} + \bar{\alpha}\frac{C_{11k}}{H_\alpha R_\alpha}\right) U_k + \left(-\bar{\beta}\frac{C_{23k}}{R_\alpha} + \bar{\beta}\frac{C_{12k}}{R_\alpha}\right) V_k + \left(-\frac{C_{11k}}{H_\alpha R_\alpha^2} - \bar{\alpha}^2 \frac{C_{55k}}{H_\alpha} - \bar{\beta}^2 C_{44k} H_\alpha + \right.$$

$$\left. \rho_k H_\alpha \omega^2\right) W_k + \left(-\bar{\alpha} C_{55k} - \bar{\alpha} C_{13k}\right) U_{k,z} + \left(-\bar{\beta} C_{44k} H_\alpha - \bar{\beta} C_{23k} H_\alpha\right) V_{k,z} + \left(\frac{C_{33k}}{R_\alpha}\right) W_{k,z} + \tag{22}$$

$$\left(C_{33k} H_\alpha\right) W_{k,zz} = 0 \,.$$

Parametric coefficients H_α are constant because the thickness coordinate z is given in the middle of each k mathematical layer. The system of Eqs.(20)-(22) is written in a compact form by introducing constant coefficients A_{sk} for each block $()$ with s from 1 to 19:

$$A_{1k} U_k + A_{2k} V_k + A_{3k} W_k + A_{4k} U_{k,z} + A_{5k} W_{k,z} + A_{6k} U_{k,zz} = 0 \,, \tag{23}$$

$$A_{7k} U_k + A_{8k} V_k + A_{9k} W_k + A_{10k} V_{k,z} + A_{11k} W_{k,z} + A_{12k} V_{k,zz} = 0 \,, \tag{24}$$

$$A_{13k} U_k + A_{14k} V_k + A_{15k} W_k + A_{16k} U_{k,z} + A_{17k} V_{k,z} + A_{18k} W_{k,z} + A_{19k} W_{k,zz} = 0 \,. \tag{25}$$

Eqs.(23)-(25) are a system of three second order differential equations. This system can be reduced to a system of first order differential equations [43]-[46]:

$$\begin{bmatrix} A_{6k} & 0 & 0 & 0 & 0 & 0 \\ 0 & A_{12k} & 0 & 0 & 0 & 0 \\ 0 & 0 & A_{19k} & 0 & 0 & 0 \\ 0 & 0 & 0 & A_{6k} & 0 & 0 \\ 0 & 0 & 0 & 0 & A_{12k} & 0 \\ 0 & 0 & 0 & 0 & 0 & A_{19k} \end{bmatrix} \begin{bmatrix} U_k \\ V_k \\ W_k \\ U_k' \\ V_k' \\ W_k' \end{bmatrix}' = \begin{bmatrix} 0 & 0 & 0 & A_{6k} & 0 & 0 \\ 0 & 0 & 0 & 0 & A_{12k} & 0 \\ 0 & 0 & 0 & 0 & 0 & A_{19k} \\ -A_{1k} & -A_{2k} & -A_{3k} & -A_{4k} & 0 & -A_{5k} \\ -A_{7k} & -A_{8k} & -A_{9k} & 0 & -A_{10k} & -A_{11k} \\ -A_{13k} & -A_{14k} & -A_{15k} & -A_{16k} & -A_{17k} & -A_{18k} \end{bmatrix} \begin{bmatrix} U_k \\ V_k \\ W_k \\ U_k' \\ V_k' \\ W_k' \end{bmatrix} \,.$$
$$\tag{26}$$

Eq.(26) can be written in a compact form for a generic k layer:

$$\boldsymbol{D}_k \frac{\partial \boldsymbol{U}_k}{\partial z} = \boldsymbol{A}_k \boldsymbol{U}_k \,, \tag{27}$$

7

where $\frac{\partial \boldsymbol{U}_k}{\partial z} = \boldsymbol{U}'_k$ and $\boldsymbol{U}_k = [U_k \ V_k \ W_k \ U'_k \ V'_k \ W'_k]$. Eq.(27) can be written as:

$$\boldsymbol{U}'_k = \boldsymbol{A}^*_k \, \boldsymbol{U}_k \,, \tag{28}$$

with $\boldsymbol{A}^*_k = \boldsymbol{D}^{-1}_k \boldsymbol{A}_k$. The solution of Eq.(28) is:

$$\boldsymbol{U}_k(z_k) = exp(\boldsymbol{A}^*_k z_k)\boldsymbol{U}_k(0) \quad \text{with} \quad z_k \ \epsilon \ [0, h_k] \,, \tag{29}$$

where z_k is the thickness coordinate of each k layer from 0 at the bottom to h_k at the top.

If we consider N_L layers, $N_L - 1$ transfer matrices $\boldsymbol{T}_{k-1,k}$ must be calculated by using for each interface the following conditions for interlaminar continuity of displacements and transverse shear/normal stresses:

$$u^b_k = u^t_{k-1} \,, \quad v^b_k = v^t_{k-1} \,, \quad w^b_k = w^t_{k-1} \,, \tag{30}$$

$$\sigma^b_{zzk} = \sigma^t_{zzk-1} \,, \quad \sigma^b_{\alpha zk} = \sigma^t_{\alpha zk-1} \,, \quad \sigma^b_{\beta zk} = \sigma^t_{\beta zk-1} \,, \tag{31}$$

each displacement and transverse stress component at the top (t) of the k-1 layer is equal to displacements and transverse stress components at the bottom (b) of the k layer. Eqs.(30)-(31) in compact form are:

$$\boldsymbol{U}^b_k = \boldsymbol{T}_{k-1,k}\boldsymbol{U}^t_{k-1} \,. \tag{32}$$

The calculated $\boldsymbol{T}_{k-1,k}$ matrices allow vector $\boldsymbol{U}$ at the bottom (b) of the k layer with vector $\boldsymbol{U}$ at the top (t) of the $k-1$ layer to be linked. The structures are simply supported and free stresses at the top and at the bottom, this feature means:

$$\sigma_{zz} = \sigma_{\alpha z} = \sigma_{\beta z} = 0 \quad \text{for} \quad z = 0, h \,, \tag{33}$$

$$w = v = 0, \ \sigma_{\alpha\alpha} = 0 \quad \text{for} \quad \alpha = 0, a \,, \tag{34}$$

$$w = u = 0, \ \sigma_{\beta\beta} = 0 \quad \text{for} \quad \beta = 0, b \,. \tag{35}$$

The combination of Eqs. (28), (29), (32) and (33)-(35) leads to the following system (details can be found in [43] and [44]):

$$\begin{bmatrix} \boldsymbol{E} \end{bmatrix} \begin{bmatrix} \boldsymbol{U}^b_1 \end{bmatrix} = \begin{bmatrix} 0 \end{bmatrix} \,. \tag{36}$$

Matrix $\boldsymbol{E}$ has always (6×6) dimension, independently from the number N_L of mathematical layers, even if the method uses a layer-wise approach. The free vibration analysis means to find the non-trivial solution of $\boldsymbol{U}_1^b$ (displacement at the bottom of the layer 1) in Eq.(36) by imposing the determinant of matrix $\boldsymbol{E}$ equals zero:

$$det[\boldsymbol{E}] = 0 \,. \tag{37}$$

Eq.(37) means to find the roots of an higher order polynomial in $\lambda = \omega^2$. For each pair of half-wave numbers (p, q) a certain number of circular frequencies are obtained depending on the order N chosen for each exponential matrix in Eq.(29) and the number N_L of mathematical layers.

3 Results

The preliminary assessment considers a simply supported Single-Walled Carbon NanoTube (SWCNT) for the beam analysis shown in Simsek [33] and Aydogdu [35] . The equivalent elastic cylinder has a very small diameter/thickness ratio, for this case the use of classical 2D shell models could exhibit some difficulties. Frequencies are also investigated for different length/diameter ratios, however beam models may be inappropriate for short SWCNTs. After the preliminary validation, the 3D shell model is used to investigate the natural frequencies of several SWCNTs with different geometries (armachair, zigzag, general chirality) and length/radius ratios.

3.1 Preliminary assessment

The SWCNT is simply supported, the equivalent elastic cylinder has properties as indicated in Simsek [33]. The equivalent Young modulus is $E = 1TPa$ with Poisson ratio $\nu = 0.3$, the effective thickness considered for this Young modulus value is $h = 0.35nm$. The mass density is $\rho = 2300kg/m^3$. The external diameter of the cylinder is $d_e = 1nm$, this value means a ratio d_e/h=2.86 which requests the use of beam models. Some difficulties may arise when classical 2D shell models are used for the analysis of such cylinders. The use of very refined 2D shell models (see Cinefra et al. [36]) or 3D exact shell models can overcome this limitation. The radius of curvature in α direction, referred to the mid-surface, is $R_\alpha = d_e/2 - h/2 = 0.325nm$. The dimension in α direction is $a = 2\pi R_\alpha$ and the b dimension is $L = 5nm$, $10nm$, $20nm$, $50nm$ and $100nm$ for ratios $L/d_e = 5$, 10, 20, 50 and 100, respectively. Table 1 gives the first three circular frequencies $\bar{\omega} = \omega L^2 \sqrt{\frac{\rho A}{EI}}$ (where A is the area of the ring and I is the moment of inertia of the ring) for short and long simply supported cylinders

with different L/d_e ratios. The first three non-dimensional circular frequencies are obtained with an imposed half-wave number p=2 in α direction and half-wave numbers q in β direction equal to 1,2 and 3. Beam models correctly work for long and moderately long cylinders. However, shell models give correct results for both long and short cylinders. The Euler-Bernoulli Beam Model (EBM) was proposed in Simsek [33] and Aydogdu [35] for the first three frequencies for ratios L/d_e=10, 20, 50. The same cases were also investigated in [35] by means of the Timoshenko Beam Model (TBM). TBM gives more accurate results than EBM because it includes the effects of transverse shear deformation and rotary inertia. However, TBM shows some problems for second and third frequency in the case of short SWCNTs (L/d_e=10). The 3D shell model gives satisfactory results for both long and short SWCNTs and it also allows for the vibration analysis of cylinders with small diameter/thickness ratios. For these small ratios, classical 2D shell models could exhibit some difficulties. Table 1 shows that the TB model gives similar results to the 3D shell model, while the EB model produces larger differences. The TB model has some difficulties for short SWCNTs. Additional results from the 3D shell model are recorded in Table 1 (they were not obtained in [33] and [35] via beam models). They show a complete overview of the SWCNT behavior and they can be used as a benchmark for the validation of future 1D beam and 2D shell models. Additional results for very short and very long SWCNTs have also been included. Scientists involved in beam and shell model analyses of SWCNTs can try to complete this table. After this assessment, the 3D shell model can be considered as validated and it can be used with confidence for future analyses.

3.2 Free vibrations of SWCNTs

In the previous assessment, the effective wall thickness h of the single-walled carbon nanotube was assumed to be equal to the inter-planar spacing of graphite layers (0.35 nm) and the mechanical properties were consequently calculated (Young modulus and Poisson ratio). The choice of this thickness value gives the equivalent mechanical properties. In the literature, there are many dissenting opinions about the mechanical characterization of carbon nanotubes. The present paper does not discuss these aspects, but it proposes a 3D model which is able to validate future continuum approaches based on 1D beam and 2D shell models. The choice of $h = 0.35nm$ gives cylinders which are very hard to analyze correctly. Different choices (with smaller thicknesses but consequently higher values of Young modulus) are possible for benchmarks with different behaviors and problems. The SWCNTs can have different geometries depending on the chiral vector $\overrightarrow{C_h} = n\overrightarrow{a_1} + m\overrightarrow{a_2}$ which also gives different radius

values (see Fig. 2 and Table 2 for further details about armachair, zigzag and general chirality CNTs). Chen and Cao [6] proposed different continuum approaches for CNT analysis, they gave a completely different value for the thickness wall h. This value was $h = 0.08nm$ that means an effective Young modulus $E = 6.85TPa$ and Poisson ratio $\nu = 0.19$. The continuum models proposed in [6] used these mechanical properties for CNT analysis. The comparison of these results with those obtained via the Molecular Dynamic (MD) analysis has always shown a difference which is less than 5%. For this reason, these properties have been used for the new benchmarks proposed in this section by means of the 3D exact model. Table 2 shows the radius of curvature r and the number of atoms for several SWCNT configurations (armachair with $n = m$, zigzag with $(n,0)$ and general chirality with $n \neq m$). The mass density ρ is not defined because the circular frequencies are given in a non-dimensional form related to ρ ($\omega^* = \omega L \sqrt{\frac{\rho}{E}}$). Several length/radius ratios (L/r) are proposed for each SWCNT, $r = R_\alpha$ is considered as the radius of curvature in the α direction with respect to the mid-surface. Table 3 shows the circular frequencies for each SWCNT described in Table 2 and Fig. 2 with length/radius ratios $L/r = 20, 25, 30, 35$. The frequencies are obtained for a half-wave number in α direction p=2 (the cylinder is closed in this direction and only even p values are possible) and half-wave numbers in β direction q from 1 to 5. For each SWCNT (armachair, zigzag and general chirality CNT) the non-dimensional circular frequencies (the first five vibration modes) decrease as the length L of CNT increases (bigger values of the L/r ratio). A longer cylinder is less rigid than the same cylinder with a shorter length L. The armachair SWCNTs (n=m) have frequencies which decrease as the value n=m increases, this feature is due to the fact that armachair CNTs with higher values of n=m have bigger radii of curvature (less rigid cylinders). This behavior is confirmed for each vibration mode (from the first to the fifth one) and for each L/r ratio. Zigzag SWCNTs (m=0) have a radius of curvature that increases with the n value (consequently the length also increases because of the L/r ratio) and the behavior is the same as that seen for the armachair CNTs. The general chirality (8,4) SWCNT has a behavior similar to that obtained for the (6,6) armachair SWCNT because the radii of curvature are almost the same. Fig. 3 summarizes some of the results given in Table 3. It shows the non-dimensional circular frequencies for armachair and zigzag SWCNTs in relation to the L/r ratio. Each non-dimensional circular frequency decreases as the L/r ratio increases. These considerations are valid for both armachair (5,5) and zigzag (16,0) SWCNTs as shown in Fig. 3.

The considerations shown in the present analysis are useful for the validation of future continuum approaches applied to vibration analysis of SWCNTs (both 1D beam and 2D shell models). The main

limitation of this paper is that the elastic properties do not change when the chirality of the SWCNT is modified (only the geometry changes). This limitation can be overcome by the use of an MD simulation that supports the present 3D exact analysis.

4   Conclusions

The present paper has proposed an exact 3D elasticity model to analyze free vibrations of Single-Walled Carbon NanoTubes (SWCNTs). The continuum approach was used by introducing an equivalent elastic isotropic cylinder in place of the discrete molecular structure of SWCNTs. The exact solution is proposed for simply supported cylinders. Several types of SWCNTs were considered such as armachair, zigzag and general chirality ones. Different radius/thickness and length/radius ratios have been considered in the analysis to show the limitations of 1D and 2D models. 1D beam models correctly work for long or moderately long cylinders (higher values of length/radius ratio). For short cylinders (smaller values of length/radius ratio) the use of 2D shell or 3D models is necessary. Classical 2D shell models can exhibit some difficulties for shells with small values of radius/thickness ratio, in this case the use of refined 2D shell models or 3D elasticity models is required. The present 3D exact elastic model could be used as a reference solution for the validation of 1D beam and 2D shell models applied to the vibration analysis of SWCNTs. The author is aware of the limitations of continuum mechanics models, and future work will be performed to integrate a molecular dynamic analysis with the present 3D exact model.

References

[1] Iijima S. Helical microtubules of graphitic carbon. Nature 1991; 354: 56-58.

[2] Valavala PK, Odegard GM. Modeling techniques for determination of mechanical properties of polymer nanocomposites. Rev Adv Mater Sci 2005; 9: 34-44.

[3] Rouainia G, Djeghaba K. Evaluation of Young's modulus of single walled carbon nanotube (SWNT) reinforced concrete composite. J Eng Appl Sci 2008; 3: 504-515.

[4] Wang CY, Zhang LC. A critical assessment of the elastic properties and effective wall thickness of single-walled carbon nanotubes. Nanotechnology 2008; 19: 1-5.

[5] Qian D, Wagner GJ, Liu WK, Yu MF, Ruoff RS. Mechanics of carbon nanotubes. Appl Mech Rev 2002; 55: 495-533.

[6] Chen X, Cao G. A structural mechanics study of single-walled carbon nanotubes generalized from atomistic simulation. Nanotechnology 2006; 17: 1004-1015.

[7] Hu YG, Liew KM, Wang Q. Modeling of vibrations of carbon nanotubes. Procedia Engineering 2012; 31: 343-347.

[8] Ansari R, Ajori S, Arash B. Vibrations of single- and double-walled carbon nanotubes with layerwise boundary conditions: A molecular dynamics study. Curr Appl Phys 2012; 12: 707-711.

[9] Chowdhury R, Adhikari S, Wang CY, Scarpa F. A molecular mechanics approach for the vibration of single-walled carbon nanotubes. Comp Mater Sci 2010; 48: 730-735.

[10] Das SL, Mandal T, Gupta SS. Inextensional vibration of zig-zag single-walled carbon nanotubes using nonlocal elasticity theories. Int J Solids Struct 2013; 50: 2792-2797.

[11] Zhang YY, Wang CM, Tan VBC. Assessment of Timoshenko beam models for vibrational behavior of single-walled carbon nanotubes using molecular dynamics. Adv Appl Math Mech 2009; 1: 89-106.

[12] Arghavan S, Singh AV. On the vibrations of single-walled carbon nanotubes. J Sound Vib 2011; 330: 3102-3122.

[13] Gupta A, Sharma SC, Harsha SP. Vibration analysis of carbon nanotubes based mass sensor using different boundary conditions. Int J Mech Eng 2012; 2: 8-12.

[14] Mir M, Hosseini A, Majzoobi GH. A numerical study of vibrational properties of single-walled carbon nanotubes. Comp Mater Sci 2008; 43: 540-548.

[15] Yan Y, Shi G, Zhao P. Frequency study of single-walled carbon nanotubes based on a space-frame model with flexible connections. J Comput 2011; 6: 1125-1130.

[16] Aydogdu M. Axial vibration of the nanorods with the non local continuum rod model. Physica E 2009; 41: 861-864.

[17] Yan JW, Liew KM, He LH. Free vibration analysis of single-walled carbon nanotubes using a higher-order gradient theory. J Sound Vib 2013; 332: 3740-3755.

[18] Vodenitcharova T, Zhang LC. Effective wall thickness of a single-walled carbon nanotube. Phys Rev B 2003; 68: 1-4.

[19] Odegard GM, Gates TS, Nicholson LM, Wise KE. Equivalent-continuum modeling of nano-structured materials. Compos Sci Technol 2002; 62: 1869-1880.

[20] Lee U, Oh H. Evaluation of the structural properties of single-walled carbon nanotubes using a dynamic continuum modeling method. Mech Adv Mater Struc 2008; 15: 79-87.

[21] Zhang LC. On the mechanics of single-walled carbon nanotubes. J Mater Process Tech 2009; 209: 4223-4228.

[22] Araújo dos Santos JV. Effective elastic moduli evaluation of single walled carbon nanotubes using flexural vibrations. Mech Adv Mater Struc 2011; 18: 262-271.

[23] Azrar A, Azrar L, Aljinaidi AA. Length scale effect analysis on vibration behavior of single walled carbon nanotubes with arbitrary boundary conditions. Rev Mec Appl Theor 2011; 2: 475-485.

[24] Benzair A, Tounsi A, Besseghier A, Heireche H, Moulay N, Boumia L. The thermal effect on vibration of single-walled carbon nanotubes using nonlocal Timoshenko beam theory. J Phys D: Appl Phys 2008; 41: 1-10.

[25] Demir C, Civalek O, Akgöz B. Free vibration analysis of carbon nanotubes based on shear deformable beam theory by discrete singular convolution technique. Math Comput Appl 2010; 15: 57-65.

[26] Foda MA. Steady state vibration analysis and mitigation of single-walled carbon nanotubes based on nonlocal Timoshenko beam theory. Comp Mater Sci 2013; 71: 38-46.

[27] Horng TL. Transverse vibration analysis of single-walled carbon nanotubes embedded in an elastic medium using Bernoulli-Fourier method. J Surf Eng Mat Adv Tech 2012; 2: 203-209.

[28] Ming L, Huiming Z. Small scale effect on thermal vibration of single-walled carbon nanotubes with nonlocal boundary condition. Res J App Sci Eng Tech 2013; 5: 2729-2733.

[29] Swain A, Roy T, Nanda PK. Vibration behaviour of single walled carbon nanotube using finite element. Int J Theor Appl Res Mech Eng 2013; 2: 129-133.

[30] Wang B, Deng ZC, Zhang K. Nonlinear vibration of embedded single-walled carbon nanotube with geometrical imperfection under harmonic load based on nonlocal Timoshenko beam theory. Appl Math Mech 2013; 34: 269-280.

[31] Wang BL, Wang KF. Vibration analysis of embedded nanotubes using nonlocal continuum theory. Compos Part B-Eng 2013; 47: 96-101.

[32] Soltani P, Kassaei A, Taherian MM, Farshidianfar A. Vibration of wavy single-walled carbon nanotubes based on nonlocal Euler Bernoulli and Timoshenko models. Int J Adv Struct Eng 2012; 4: 1-10.

[33] Simsek M. Vibration analysis of a single-walled carbon nanotube under action of a moving harmonic load based on nonlocal elasticity theory. Physica E 2010; 43: 182-191.

[34] Murmu T, Pradhan SC. Buckling analysis of a single-walled carbon nanotube embedded in an elastic medium based on nonlocal elasticity and Timoshenko beam theory and using DQM. Physica E 2009; 41: 1232-1239.

[35] Aydogdu M. A general non local beam theory: Its application to nanobeam bending, buckling and vibration. Physica E 2009; 41: 1651-1655.

[36] Cinefra M, Carrera E, Brischetto S. Refined shell models for the vibration analysis of multiwalled carbon nanotubes. Mech Adv Mater Struc 2011; 18: 476-483.

[37] Wang CY, Zhang LC. An elastic shell model for characterizing single-walled carbon nanotubes. Nanotechnology 2008; 19: 1-6.

[38] Alibeigloo A, Shaban M. Free vibration analysis of carbon nanotubes by using three-dimensional theory of elasticity. Acta Mech 2013; 224: 1415-1427.

[39] Mikhasev M. On localized modes of free vibrations of single-walled carbon nanotubes embedded in nonhomogeneous elastic medium. Z Angew Math Mech 2013; 1-12.

[40] Dong K, Zhu SQ, Wang X. Wave propagation in multiwall carbon nanotubes embedded in a matrix material. Compos Struc 2008; 82: 1-9.

[41] Li R, Kardomateas GA. Vibration characteristics of multiwalled carbon nanotubes embedded in elastic media by a nonlocal elastic shell model. J Appl Mech 2007; 74: 1087-1094.

[42] Yao X, Han Q. Torsional buckling and postbuckling equilibrium path of double-walled carbon nanotubes. Compos Sci Technol 2008; 68: 113-120.

[43] Brischetto S. Three-dimensional exact free vibration analysis of spherical, cylindrical and flat one-layered panels. Submitted 2013.

[44] Brischetto S. An exact three-dimensional solution for free vibrations of multilayered composite and sandwich plates and shells. Submitted 2013.

[45] Messina A. Three dimensional free vibration analysis of cross-ply laminated plates through 2D and exact models. In: Proceedings of Third International Conference on Integrity, Reliability and Failure. Porto (Portugal), July, 2009. p. 1-18.

[46] Soldatos KP, Ye J. Axisymmetric static and dynamic analysis of laminated hollow cylinders composed of monoclinic elastic layers. J Sound Vib 1995; 184: 245-259.
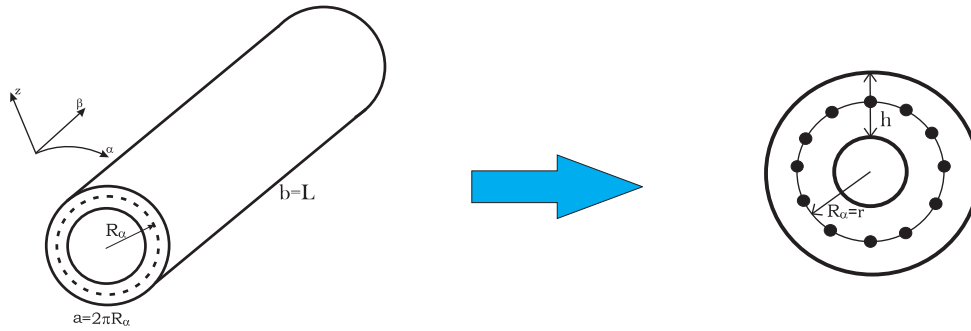
Figure 1: Notation, reference system and continuum approach for a Single-Walled Carbon NanoTube (SWCNT).
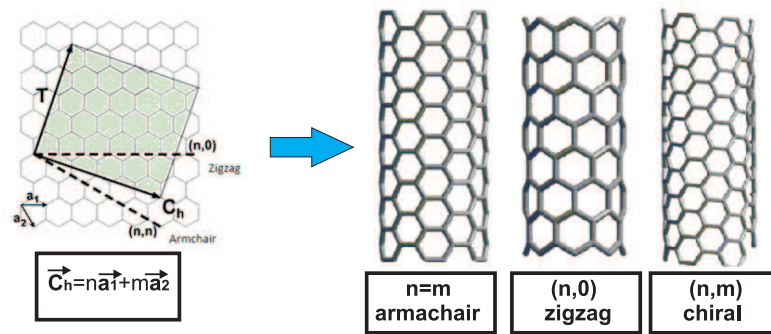

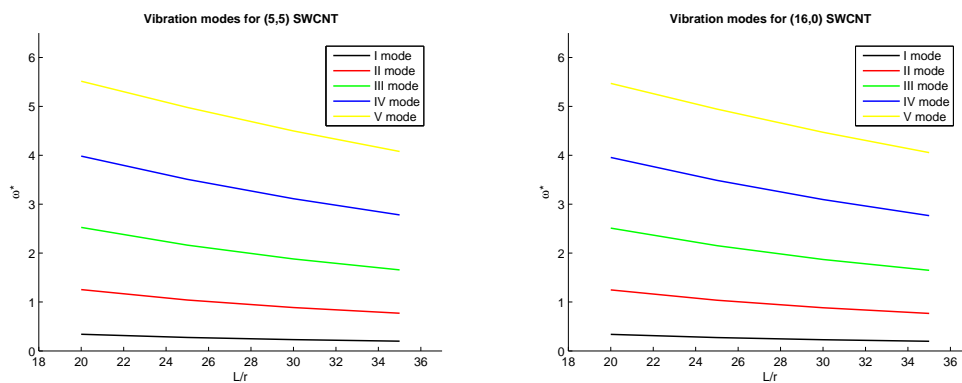Figure 2: Chiral vector for armachair, zigzag and general chirality single-walled carbon nanotubes.

Figure 3: Benchmark, non-dimensional circular frequencies ω^* for armachair (5,5) (on the left) and zigzag (16,0) (on the right) SWCNTs versus L/r ratio.

mode (p,q)	3D Shell	EBM[33],[35]	TBM[35]
	$L/d_e = 5$		
I (2,1)	9.3481	. . .	. . .
II (2,2)	32.917	. . .	. . .
III (2,3)	63.917	. . .	. . .
	$L/d_e = 10$		
I (2,1)	9.7295	9.8696	9.7443
II (2,2)	37.392	39.478	36.841
III (2,3)	79.361	88.826	57.450
	$L/d_e = 20$		
I (2,1)	9.8356	9.8696	9.8381
II (2,2)	38.918	39.478	38.964
III (2,3)	86.072	88.826	85.748
	$L/d_e = 50$		
I (2,1)	9.8638	9.8696	9.8645
II (2,2)	39.392	39.478	39.398
III (2,3)	88.375	88.826	88.415
	$L/d_e = 100$		
I (2,1)	9.8487	. . .	. . .
II (2,2)	39.488	. . .	. . .
III (2,3)	88.752	. . .	. . .

Table 1: Preliminary assessment: comparison between present 3D shell model and beam models (Euler-Bernoulli Beam Model (EBM) and Timoshenko Beam Model (TBM)) proposed in [33] and [35]. First three non-dimensional circular frequencies $\bar{\omega}$ for different L/d_e ratios. p and q are the imposed half-wave numbers.

SWCNT (n,m)	(5,5)	(6,6)	(7,7)	(8,8)	(10,0)	(12,0)	(14,0)	(16,0)	(8,4)
r(nm)	0.338	0.405	0.473	0.540	0.390	0.468	0.546	0.624	0.413
n. atoms	1040	1248	1456	1664	1200	1440	1680	1920	1200

Table 2: Geometry and properties (radius of curvature and number of atoms) for SWCNTs used in the present paper and in Chen and Cao [6].

L/r	I (2,1)	II (2,2)	III (2,3)	IV (2,4)	V (2,5)
			armachair (5,5)		
20	0.3404	1.2535	2.5261	3.9825	5.5138
25	0.2754	1.0413	2.1635	3.5088	4.9781
30	0.2309	0.8870	1.8802	3.1114	4.4967
35	0.1987	0.7709	1.6564	2.7815	4.0771
			armachair (6,6)		
20	0.3397	1.2507	2.5199	3.9712	5.4953
25	0.2748	1.0390	2.1585	3.4999	4.9641
30	0.2304	0.8851	1.8760	3.1040	4.4851
35	0.1982	0.7692	1.6528	2.7751	4.0671
			armachair (7,7)		
20	0.3392	1.2489	2.5160	3.9643	5.4838
25	0.2744	1.0376	2.1554	3.4945	4.9554
30	0.2301	0.8839	1.8734	3.0994	4.4780
35	0.1980	0.7682	1.6505	2.7711	4.0610
			armachair (8,8)		
20	0.3389	1.2478	2.5135	3.9598	5.4764
25	0.2742	1.0367	2.1534	3.4904	4.9498
30	0.2299	0.8832	1.8717	3.0965	4.4734
35	0.1978	0.7676	1.6491	2.7686	4.0571
			zigzag (10,0)		
20	0.3398	1.2512	2.5210	3.9733	5.4986
25	0.2749	1.0394	2.1594	3.5015	4.9666
30	0.2305	0.8854	1.8763	3.1053	4.4872
35	0.1983	0.7695	1.6534	2.7762	4.0689
			zigzag (12,0)		
20	0.3392	1.2490	2.5162	3.9647	5.4845
25	0.2744	1.0377	2.1556	3.4948	4.9559
30	0.2301	0.8840	1.8735	3.0997	4.4784
35	0.1980	0.7683	1.6507	2.7714	4.0614
			zigzag (14,0)		
20	0.3389	1.2477	2.5134	3.9595	5.4759
25	0.2742	1.0366	2.1533	3.4907	4.9494
30	0.2299	0.8831	1.8716	3.0963	4.4730
35	0.1978	0.7675	1.6490	2.7684	4.0568
			zigzag (16,0)		
20	0.3387	1.2469	2.5115	3.9561	5.4703
25	0.2740	1.0359	2.1518	3.4880	4.9452
30	0.2298	0.8825	1.8703	3.0941	4.4696
35	0.1977	0.7670	1.6479	2.7765	4.0538
			general chirality (8,4)		
20	0.3396	1.2504	2.5193	3.9703	5.4936
25	0.2747	1.0388	2.1581	3.4992	4.9628
30	0.2304	0.8849	1.8756	3.1033	4.4841
35	0.1982	0.7691	1.6524	2.7745	4.0663

Table 3: Present 3D shell model, frequencies in non-dimensional circular form ω^* for different SWCNTs and L/r ratios. Imposed half-wave numbers p=2 in α direction and q=1,...,5 in β direction.